SPECIAL INVITED PAPER
ON VOLCANO AND UNDERGROUND MUOGRAPHY FOR SEAMLESS VISUALIZATION OF THE SUBSURFACE DENSITY STRUCTURE OF THE EARTH

Hiroyuki K.M. Tanaka*[1] & Lee F. Thompson**
*Earthquake Research Institute, The University of Tokyo, Tokyo, Japan
**Department of physics and Astronomy, University of Sheffield, Sheffield, UK
(Accepted 31 May 2016; Available online 7 June 2016)

ABSTRACT

A new visualization technique called muography is capable of creating projected images of larger objects than possible with conventional x-ray radiography. The technique utilizes elementary particles called muons generated in the Earth's atmosphere, and therefore can be applied to almost every gigantic object on the Earth. A new technique for the Earth subsurface imaging/monitoring will be discussed by reviewing some of the most recent achievements of volcano and underground muography.

1. INTRODUCTION

Muography is a visualization technique that utilizes elementary particles called muons. The energy of muons generated in the atmosphere as the secondary particles of cosmic rays ranges between a few GeV to a few TeV. Sub-GeV and very high energy (VHE; >PeV) muons exist but are rare and therefore, most of them can penetrate rock from a decametric to a kilometric scale. These properties make it possible for muography to be applied to visualize the internal structures of volcanoes [Tanaka et al. 2014; Carbone et al. 2013; Lesparre et al. 2012; Carloganu et al. 2012], industrial plants [Tanaka 2013], nuclear reactors [Morishima 2015], seismic faults [Tanaka et al. 2011; Tanaka et al. 2015], ore bodies [Liu et al. 2012], caves [Hola et al. 2015], nuclear waste [D'Alessandro et al. 2014], and carbon capture and storage [Klinger et al. 2015].

E.P. George's first attempt to measure the areal density of the rock overburden with cosmic-ray muons was a pioneering work that triggered all the muographic experiments to follow [George 1955]. However he utilized the Geiger counter for his measurement and therefore could not image the density structure of the overburden. Thirteen year later L. Alvarez et al. (1970) attempted to conduct the first muographic measurement inside Chephren's pyramid in Egypt. He placed spark chambers inside the Belzoni chamber to search for hidden chambers inside the pyramid. Although the collaboration could not find a hidden chamber, they showed evidence that muography was sensitive to small variations in the areal density along the muon path by detecting the 2-m thick cap rock existing above more than 100-m thick limestone block.

As long as the muon tracker is located beneath the target of interest, muography can produce a projected image of the density anomaly. When convex topography (such as volcanoes) is targeted, the tracker can

[1] ht@riken.jp

be placed at the foot of the target. When underground structures are imaged, the tracker should be installed in appropriately situated underground tunnels or boreholes. Once volcano and underground muography has become more developed, seamless visualization of the subsurface density structure of the Earth will be possible. In this paper, recent progress in volcano and underground muography is briefly reviewed with some successful imaging examples.

2. PRINCIPLE

Muons are generated by the interaction between the primary cosmic rays and atmospheric nuclei. The galactic magnetic field traps primary cosmic rays and these particles diffuse out to the Earth. Due to the random fluctuations of the field strength, the initial directional information of the cosmic rays has been completely lost by the time they arrive at the Earth. However, the muon energy spectrum has a zenith-angle dependence. This comes from the zenith-angle dependence of the atmosphere's thickness and the mean free path (MFP) of the secondary mesons (pions and kaons that eventually decay into muons) in the atmosphere. Vertical pions and kaons collide more with the atmospheric nuclei before they decay in comparison to the horizontal pions and kaons that tend to decay before further collisions. Such a difference in the meson's interaction produces more muons with lower energies in the vertical direction, and less muons with higher average energies in the horizontal direction. Once muons are produced, most of them reach the ground surface before decay (τ~2.2 μs) due to the relativistic effect. The zenith-angle dependence of the muon energy spectrum at sea level has been experimentally measured [Jokisch et al. 1979; Matsuno et al. 1984; Allkofer et al. 1985; Haino et al. 2004; Achard et al. 2004] and numerically modeled [Bull et al. 1965; Matsuno et al. 1984; Bugaev et al. 1998; Gaisser and Stanev 2008] by researchers. The integrated vertical muon flux is proportional to $E^{-2.2}$ in the energy region between 50 and 200 GeV.

Muons lose their energy in matter via the following four processes: ionization, bremsstrahlung, direct pair production, and photo-nuclear interactions. Because muons are more than 200 times heavier than electrons, radiative processes (such as bremsstrahlung) are strongly suppressed and as a result, the muon range is longer than the electron range with the same incident energies. For example, 40 GeV and 200 GeV corresponds to the muon range of 180 and 740 m.w.e respectively whereas electrons cannot penetrate more than 100 radiation lengths (X_0) that is equivalent to ~20-m rock. In particular, below the critical energy of 708 GeV in SiO_2, the ionization process is the main cause of the muon's energy loss [Olive et al. 2014], and thus muons of a given energy have an almost unique range. For example, the contribution of the radiative process to the muon's energy loss is less than 5% at 100 GeV. Because the muon's energy loss rate calculated by using the high energy approximation of the Bethe-Bloch equation [Adair and Kasha 1976] is a function of energy but has the slow logarithmic dependence, the range and energy have a nearly linear relationship below the critical energy threshold.

By combining the zenith-angle dependence of the muon's energy spectrum and the muon range representing an almost single-valued function of the incident energy, we obtain the relationship between the rock areal density and muon flux after passing through matter as a function of the muon's arriving zenith angle (Fig. 1). The areal density can then be derived by knowing the active area of the muon tracker, its angular resolution, measurement time, number of muon events, and their arriving angles. Average density along the muon path is calculated by dividing the derived areal density by the geometrical muon's path length that can be obtained from the observation location and the topographic map of the target.

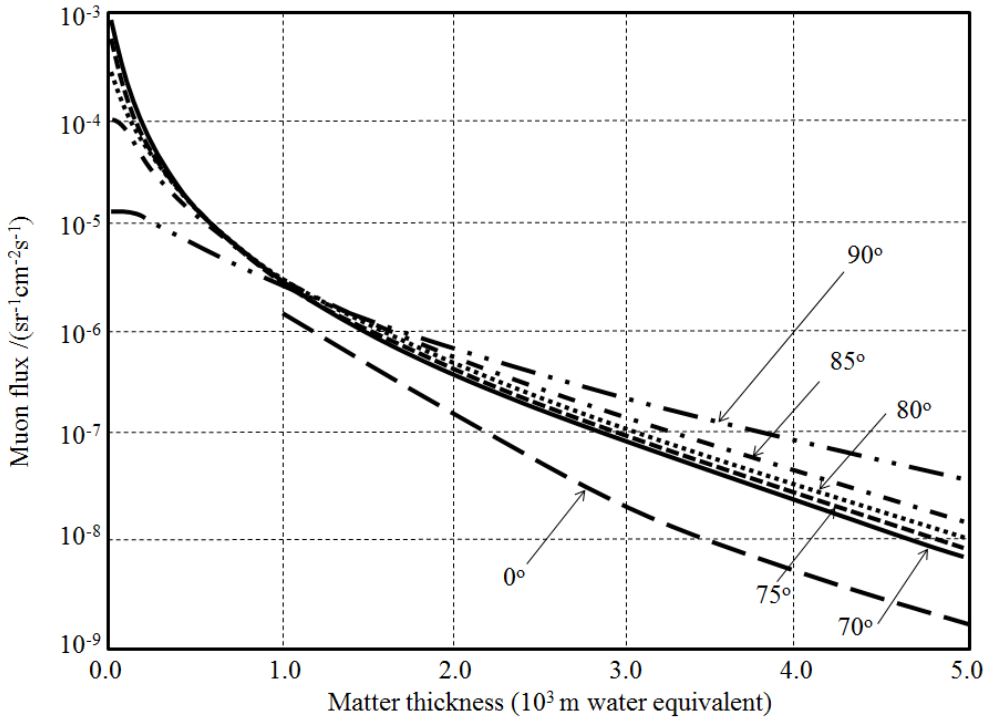

Fig. 1. Muon flux after passing through the given thickness of matter. The muon's arriving angles from zenith are indicated.

3. VOLCANO MUOGRAPHY

3.1. Technologies

Near horizontal muons are used for volcano muography. The muon tracker is placed at the foot of mountain and record the number and direction of the muons after passing through the mountain. Two major muography techniques have been used for measuring volcanoes with muons. Film muography utilizes the technique of nuclear emulsions, and therefore the observation does not require electric power. Real-time muography utilizes scintillation and gaseous detectors, and it enables us to monitor volcanic activities in real time.

3.1.1 Film muography

When charged particles pass through the nuclear emulsion which contain AgBr micro-crystals, the crystal color turns black along their trajectories after development. After the exposure and development of the nuclear emulsion, the 3 dimensional distributions of the blackened crystals are visualized by using the scanning microscope [Bozza et al. 2014]. For the purpose of muography, only the linear trajectories are selected.

The nuclear emulsion integrates all muon events after it is produced, and therefore, at least 2 independent films are used as a muon tracker in order to distinguish the events before and after the observation. Only the events that pass through both of the films are considered to be legitimate muon events, while the events that do not connect between the two films are considered to be background events [Tanaka et al. 2007].

In field muography, the nuclear emulsion is coated by rubber sheets and then shielded by metal plates. The metal plates are used as a radiation shield. Volcanic rocks are known to be a source of beta rays and they could degrade the resultant image if this radiation shield was not used. The rubber sheets are used for as a heat insulator. Without insulation, the film will directly touch the metal plate, and the expansion and contraction due to the diurnal temperature variations will cause the distortion of the resultant muographic image [Tanaka et al. 2007].

3.1.2 Real-time muography

Scintillation and gas detectors have been used as real time muography. These detectors are position sensitive and two or more detectors are used in the experiment for identification of spatially independent vertex points that are required to track the muon trajectories. With the scintillator-based muon tracker, the combination of the *X* and *Y* strips of the plastic scintillator determines the position where the muons pass the detector and since they are optically isolated, its positioning resolution equals the width of the scintillator strip. The scintillation light is converted to electric signals by using PMTs [Tanaka et al. 2009] or silicon detectors [Ambrosino et al. 2014] in order to allow the subsequent logical signal processing for tracking muons. Scintillation light is transferred to these photodetectors via the acryl light guides or wave length shift (WLS) fibers.

There are two different successful design schemes used for gas detectors: the multi wired proportional chamber (MWPC) [Hola et al. 2015] and the glass resistive plate chamber (GRPC) [Carloganu 2013]. Inside the multi wired proportional chamber (MWPC), the *X*-*Y* anode wires take on a similar role to that of the strips in a scintillation detector; these *X*-*Y* anode wires indicate the location where the muons pass the detector, and the wire spacing determines its positioning resolution. However, unlike scintillation detectors, the wires are not electrically isolated. Conventionally, it was difficult to apply the MWPC to field muography because these wires were fragile against mechanical shocks and therefore there were high risks of detector malfunction or breakage during transportation. However, recent developments in gas-based muography have enabled more mechanically robust MWPC with thicker wires and wider wire spacing. The GRPC has a similar principle for particle detection to the MWPC, however the signal pickup electrode strips are electrically isolated. The GRPC does not have fragile wires and therefore it is more robust against the mechanical shock. Recent developments in the micromesh technology will enable us to perform high definition muography in real time in the future [Chefdeville et al. 2015].

3.2 Applications

Following first successful visualization of the volcano's interior with muography in 2006 [Tanaka et al. 2007], film muography to achieve high angular resolution without requiring electric power has enabled us to produce a static but high definition image even under the harsh conditions of field muography.

Stromboli (926 m a.s.l.), Italy is one of the most active volcanoes in the world. The pyroclastic flow has recurrently occurred on the northwest flank. This region is called Sciara del Fuoco, meaning "stream of fire" and is the remnant of the past mountain collapse. Commercial electricity was not available near

the vent, and the diameter of the conduit was estimated to be thin (~10 m in diameter). Therefore, nuclear emulsion was the most suitable muon tracker for the Stromboli observation. An emulsion tracker with an active area of 0.96 m^2 was placed to target a vent region that was 600 m away from the tracker position and captured the low density region near the vent area [Tioukov et al. 2014].

A real-time detector is required to visualize magma dynamics inside a volcano in order to study phenomenon such as magma convection. For instance, it was hypothesized that magma convection was the explanation for magma dynamics in the Satsuma-Iwojima volcano (704 m a.s.l.), Japan [Shinohara and Tanaka 2012]. The rhyolitic magma of Satsuma-Iwojima is viscous and therefore a thick conduit (of a few 100m in diameter) was assumed. Tanaka et al. (2009) used a real-time muography to visualize the degassing magma with a diameter of ~300m in Satsuma-Iwojima and confirmed that the sub-millimeter positioning resolution was not required to visualize Satsuma-Iwojima magma dynamics. Tanaka et al. (2014) upgraded the standard scintillator-based muon tracker by lowering the background rate and enlarging the active area. By the conclusion of the experiment the team had a sequence of images recording the ascent and descent of the magma head associated with the 2013 Satsuma-Iwojima eruption (Fig. 2).

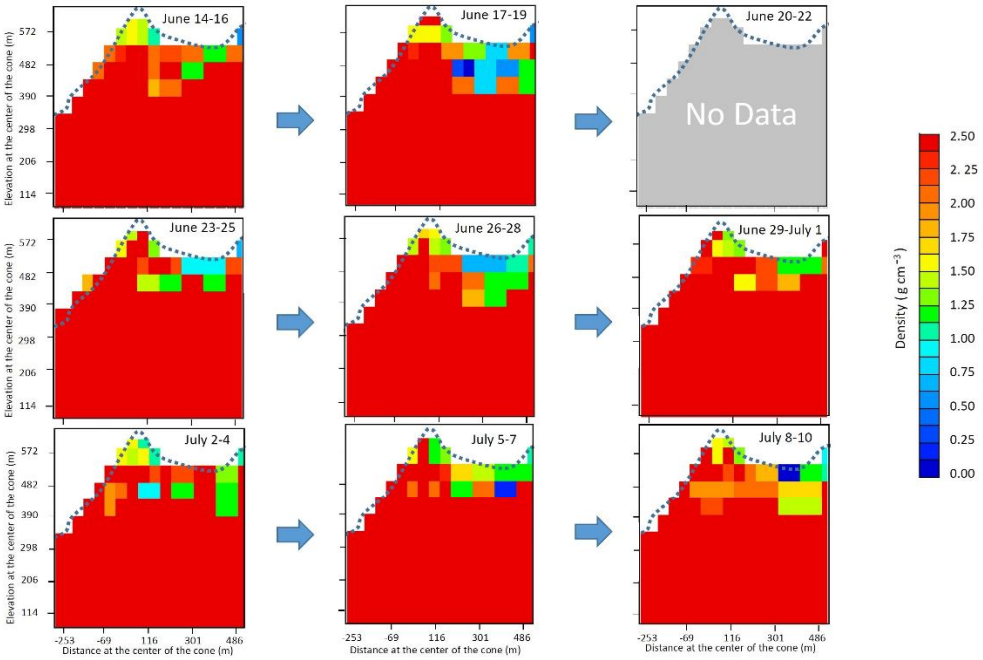

Sequence of the 2013 Satsuma-Iwojima eruption.

Date June	4	6	7	16	17	30	July 10
Column height (m)	—	300	600	400	100	200	—
Volcanic glow	—	—	—	X	—	X	—

Remarks	Lv2 eruption	Lv2 eruption
	Warning issued	Warning cancelled

Fig. 2. Time sequential muographic images taken in Satasuma-Iwojima volcano and the sequence of the 2013 Satsuma-Iwojima eruption.

A similar scintillator-based muon tracker was also used to observe La Soufrièr volcano (1234 m a.s.l.), France. The gradual increase in the transmitted muon flux after passing through the bottom part of the crater was observed, and this phenomenon preceded the activation of new vents in the summit region [Carloganu (2013)]. Not only the scintillation-based tracker but also the gas-based tracker showed a capability for application to field muography in experiments conducted at Puy de Dôme volcano (1465 m a.s.l.), France. For example, Carloganu et al. (2012) used muography to image the high density part associated with the magma intrusion at the central part of the volcano with the GRPC-based tracker.

4. UNDERGROUND MUOGRAPHY

4.1. Technologies

In order to image an underground structure, the muon detector has to be located beneath the region of interest. Underground tunnels and boreholes provide an opportunity for us to access these relevant underground regions for muography detector placement.

4.1.1. Tunnel muography

Unlike volcano muography conducted from the ground surface, underground muography utilizes near vertical muons. When the diameter of the underground tunnel is larger than a few m, the tracker prepared for volcano muography can be directly used to measure the number and arrival directions of muons after passing through the rock overburden. Scintillator and gas trackers have been used for tunnel muography. Liu et al. (2012) installed a standard segmented scintillator tracker into a mine gallery to image the zinc ore body. Hola et al. (2015) installed their MWPC-based tracker into a natural cave located underneath the Budapest, Hungary and showed the capability of the gas tracker for practical tunnel muography. In an underground tunnel the diurnal and seasonal temperature variations are smaller in comparison to the ground surface, offering better environmental conditions for operating gas trackers. A gas tracker was also utilized by Caffau et al. (1997) to explore the geological structure of Grotta Gigante, Italy. In many cases, the thickness of the overburden is thinner than the typical size of the volcanoes.

4.1.2. Borehole muography

When an underground tunnel is not available, a borehole is another choice for underground muography. Because boreholes are narrow shafts drilled in the ground, a rod-type muon tracker is required to locate it underground. The MGR (Muon Ground Radiograph) is one of the successful examples of the rod-type muon trackers used for borehole muography [Menichelli et al. 2007]. With the MGR, the combination of the signals from the spirally and vertically aligned scintillating fibers determines the two spatially independent vertex points that are used to track the muons inside the borehole. A detector with a diameter of 14 cm was inserted and collected the data at a depth of 7m from the ground surface for the Menichelli's experiment. The magnetic compass was used for identifying their tracker's direction. However, it should be noted that the soil sometimes contains a strongly magnetic minerals and can locally distort compass readings.

4.2 Applications

Underground muography has the potential to be an alternative or additional tool to supplement conventional geophysical exploration methods for mineral explorations, carbon capture and storage monitoring, and seismic fault distribution visualization.

Liu et al. (2012) inserted the portable muon tracker inside the mine gallery of the Price Mine, Canada to image the high-density zinc ore body (3.2 g/cm^3) that was embedded in the lower density rock overburden (2.7 g/cm^3). The collaboration measured the muon signals at 7 different sites in the tunnel to capture a three-dimensional image of the ore body. Muographically estimated mass and position of the ore was compared with the diamond drilling results, and they were in agreement within 7% for the mass and 1% for the position. Tanaka et al. (2015) utilized a similar portable muon detector to measure the density of the rock overburden of the traffic tunnels in Japan. Japanese traffic tunnels are densely distributed across the nation, and the subsurface density distribution revealing low density mechanical fractured zones corresponded to areas surrounded by seismic faults.

Menichelli et al. (2007) investigated the performance of their tracker by inserting the MGR inside a borehole located at the Aquileia archaeological site, Italy. By superimposing the muographic image above the archaeological map, the capability of borehole muography to detect buried construction elements became evident.

Borehole muography can also be a powerful tool for monitoring carbon capture and storage (CCS). When CO_2 is injected into an underground reservoir, the density will locally change by a few percent with respect to the surrounding rock, and it will correspond to variations of up to 1% in the areal density along the muon path [Klinger et al. 2015]. A muon tracker with an active area of 1000 m^2 will detect these changes in the muon flux due to the presence of injected CO_2 within a few months (Fig. 3). Seismic tomography and electric resistivity techniques have been conventionally used for monitoring CCS. However, these active techniques cost more than the estimated costs for performing borehole muography per unit area.

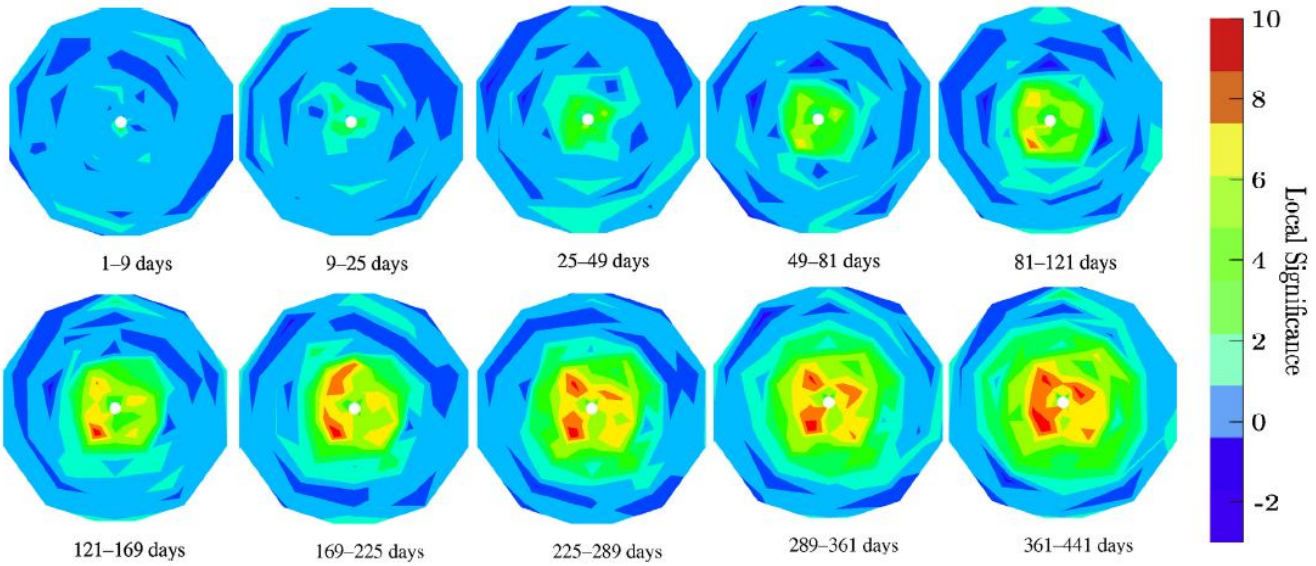

Fig. 3. Radial distribution of the statistical significance of the muon counts as a function of the measurement time. The borehole muon tracker is located at the center of the circle.

5. CONCLUSION

Underground laboratories have served important roles for cosmic ray studies. Therefore, it wasn't such a stretch of the imagination for E.P. George to decide to use an underground tunnel for his 1955 experiment. L. Alvarez et al. (1970) evolved the George's technique to a true muography technique thirteen years later. However, the technology of the time dictated that a larger space for placement of the tracker was needed inside the pyramid. Volcano muography utilizes near horizontal muons, and therefore it is not necessary to place the tracker neither inside nor underneath the volcano. The muon tracker can be placed any open space around the target. Muography with near horizontal muons has enlarged the range of choices for muographic targets, and the technique has now been applied to the industrial plants and nuclear reactors. However for underground muography, large space requirements for placement of the tracker continue to restrict potential targets. Borehole muography will remove this restriction. Borehole drilling is much more cost effective in comparison to constructing underground tunnels. Furthermore, there are a countless number of drilling holes in the world. If we can utilize boreholes by drilling as needed and taking advantage of pre-existing ones, more underground structures can be imaged. Once borehole muography is successfully developed, a more seamless muography scheme will be widened and exploration of the subsurface structure of the Earth will be possible.

REFERENCES

Achard, P. et al.: Studies of hadronic event structure in e+ e-annihilation from 30 to 209GeV with the L3 detector, *Physics Reports*, **399**, **2**, 71-174, 2004.

Adair, R.K., Kasha, H.: In: Hughes, V.W., Wu, C.S. (Eds.), *Muon Physics*, vol. 1. Academic Press, p. 323, 1976.

Allkofer, O. C. et al.: Cosmic ray muon spectra at sea-level up to 10 TeV. *Nucl. Phys. B*, **259(1)**, 1–18. 1985.

Alvarez, L.W. et al.: Search for hidden chambers in the pyramid. *Science* **167**, 832-739, 1970.

Ambrosino, F. et al.: The MU-RAY project: detector technology and first data from Mt. Vesuvius or silicon detectors, *Journal of Instrumentation*, **9**, C02029, 2014.

Bozza C. et al.: Nuclear emulsions techniques for muography. *MUOGRAPHERS 2014*, 12 November 2014, Tokyo, Japan, 2014.

Bugaev E.V. et al.: Atmospheric muon flux at sea level, underground, and underwater, *Phys. Rev. D*, **58**, 054001, 1998.

Bull, R., Nash, W.F., Rustin, B.C.: The Momentum Spectrum and Charge Ratio of I~-Mesons at Sea-Level - II, *Nuovo Cimento*, **XLA**, **2**, 365-384, 1965.

Caffau, E., Coren, F. & Giannini, G.: Underground cosmic-ray measurement for morphological reconstruction of the Grotta Gigante natural cave, *Nucl. Instrum. Methods A*, **385**, 480–488, 1997.

Carbone, D. et al.: An experiment of muon radiography at Mt. Etna (Italy). *Geophys. J. Int.* **196**, 633-643, 2013.

Carloganu C. et al.: Towards a muon radiography of the Puy de Dôme. *Geosci. Instrum. Methods Data Syst.* **2**, 55–60, 2012.

Carloganu, C.: Review of Muography in France (La Soufriere and Puy de Dome), *International Workshop on "Muon and Neutrino Radiography 2013"*, 25-26 July 2013, Tokyo, Japan, 2013.

Chefdeville, M. et al.: Micromegas for muography, the Annecy station and detectors. *Arche meeting*, 21 December 2015, Thessaloniki, Greece, 2015.

D'Alessandro, R, on behalf of the MURAVES collaboration: Muography applied to nuclear waste storage sites, *MUOGRAPHERS 2014*, 12 November 2014, Tokyo, Japan, 2014.

Gaisser T. and Stanev, T.: Cosmic Rays, *Phys. Lett. B*, **667**, 254–260, 2008.

George, E.P.: Cosmic rays measure overburden of tunnel. *Commonw. Eng.* **1955**, 455-457, 1955.

Haino, S. et al.: Measurements of primary and atmospheric cosmic-ray spectra with the BESS-TeV spectrometer. *Phys. Lett. B*, **594(1-2)**, 35–46, 2004.

Klinger, J. et al.: Simulation of muon radiography for monitoring CO_2 stored in a geological reservoir, *International Journal of Greenhouse Gas Control*, **42** 644-654, 2015.

Jokisch, H. et al.: Cosmic-ray muon spectrum up to 1 TeV at 75° zenith angle. *Phys. Rev. D*, **19(5)**, 1368–1372, 1979.

Lesparre, N. et al.: Density muon radiography of La Soufriere of Guadeloupe volcano: comparison with geological, electrical resistivity and gravity data. *Geophys. J. Int.* **190**, 1008-1019, 2012.

Liu, Z., Bryman, D., Bueno J.: Application of Muon Geotomography to Mineral Exploration, *International Workshop on "Muon and Neutrino Radiography 2012"*, 17-20 April 2012, Clermont-Ferrand, France, 2012.

Matsuno, S. et al.: Cosmic-ray muon spectrum up to 20 TeV at 89° zenith angle *Phys. Rev. D* **29** 1-23, 1984.

Menichelli, M.: A scintillating fibres tracker detector for archaeological applications, *Nucl. Instr. and Meth. A* **572**, 262–265, 2007.

Morishima, K.: Muographic investigation in Fukushima nuclear power plant. *Muography: perspective drawing in the 21st century*, 87-89, 2015.

Oláh, L. et al. High energy physics innovation for earth science from Hungary, *Muography: perspective drawing in the 21st century*, 77-85, 2015.

Olive, K.A et al.: Review of particle physics, *Chin. Phys. C*, **38**, 090001, 2014.

Shinohara, H. & Tanaka, H.K.M.: Conduit magma convection of a rhyolitic magma: Constraints from cosmic-ray muon radiography of Iwodake, Satsuma-Iwojima volcano, Japan, *Earth and Planetary Science Letters*, **349–350**, 87-97, 2012.

Tanaka, H.K.M. et al.: Radiographic visualization of magma dynamics in an erupting volcano, *Nature Communications* **5**, 3381, 2014.

Tanaka, H. K. M.: Development of stroboscopic muography, *Geosci. Instrum. Method. Data Syst.*, **2**, 41–45, 2013.

Tanaka, H. K. M. et al.: Cosmic muon imaging of hidden seismic fault zones: Raineater permeation into the mechanical fracture zone in Itoigawa-Shizuoka Tectonic Line, Japan. *Earth Planet. Sci. Lett.* **306**, 156–162, 2011.

Tanaka, H. K. M.: Muographic mapping of the subsurface density structures in Miura, Boso and Izu peninsulas, Japan. *Sci. Rep.* **5,** 1–10, 2015.

Tanaka, H. K. M. et al.: High resolution imaging in the inhomogeneous crust with cosmic-ray muon radiography: The density structure below the volcanic crater floor of Mt. Asama, Japan. *Earth Planet. Sci. Lett.* **263**, 104–113, 2007.

Tanaka, H.K.M. et al.: Cosmic-ray muon imaging of magma in a conduit: degassing process of Satsuma-Iwojima Volcano, Japan, *Geophys.Res. Lett.*, **36**, L01304, 2009.

Tioukov, V. et al.: Muography with nuclear emulsions – Stromboli and other projects, *MUOGRAPHERS 2014*, 12 November 2014, Tokyo, Japan, 2014.